Journal of Nuclear Science and Technology

ISSN: 0022-3131 (Print) 1881-1248 (Online) Journal homepage: https://www.tandfonline.com/loi/tnst20

Neutron total cross section measurements of polyethylene using time-of-flight method at KURNS-LINAC

Jaehong Lee, Jun Nishiyama, Jun-Ichi Hori, Rei Kimura, Takayuki Sako, Akira Yamada & Tadafumi Sano

To cite this article: Jaehong Lee, Jun Nishiyama, Jun-Ichi Hori, Rei Kimura, Takayuki Sako, Akira Yamada & Tadafumi Sano (2020) Neutron total cross section measurements of polyethylene using time-of-flight method at KURNS-LINAC, Journal of Nuclear Science and Technology, 57:1, 1-8, DOI: 10.1080/00223131.2019.1647894

To link to this article: https://doi.org/10.1080/00223131.2019.1647894

Published online: 12 Aug 2019.

JOURNAL OF NUCLEAR SCIENCE AND TECHNOLOGY
2020, VOL. 57, NO. 1, 1–8
https://doi.org/10.1080/00223131.2019.1647894

ARTICLE

OPEN ACCESS Check for updates

Neutron total cross section measurements of polyethylene using time-of-flight method at KURNS-LINAC

Jaehong Lee[a], Jun Nishiyama[b], Jun-Ichi Hori[a], Rei Kimura[c], Takayuki Sako[d], Akira Yamada[c] and Tadafumi Sano[a]

[a]Institute for Integrated Radiation and Nuclear Science, Kyoto University, Osaka, Japan; [b]Laboratory for Advanced Nuclear Energy, Institute of Innovative Research, Tokyo Institute of Technology, Tokyo, Japan; [c]Toshiba Energy Systems & Solutions, Kawasaki-ku Kawasaki, Kanagawa, Japan; [d]Toshiba Energy Systems & Solutions, Yokohama, Kanagawa, Japan

ABSTRACT

The neutron total cross sections of polyethylene have been measured in the energy region from 0.001 eV to 40 keV by the time-of-flight (TOF) method using the Kyoto University Institute for Integrated Radiation and Nuclear Science – Linear Accelerator (KURNS-LINAC). A ^{6}Li detector and a gas electron multiplier (GEM) detector have been used as a neutron detector, and the polyethylene plates of 0.31 and 0.20 cm thickness were employed for the neutron transmission measurement.

The present results were compared with the previous results and the evaluated data in JENDL-4.0. In the energy region below 0.01 eV, the present results are in good agreement with the data measured by Herdade *et al.* (1973) and by Granada *et al.* (1987). On the other hand, the evaluated data in JENDL-4.0 are larger than all the measured data. In the energy region from 0.035 to 0.15 eV, the data measured by Granada *et al.* and the evaluated data in JENDL-4.0 are up to about 4 ~ 6% larger than the present results.

ARTICLE HISTORY
Received 10 April 2019
Accepted 19 July 2019

KEYWORDS
Neutron total cross sections; polyethylene; time-of-flight method; KURNS-LINAC

1. Introduction

The neutron cross sections provide information about what happens to the neutrons when they pass with atoms of the material. For this reason, the accurate neutron cross sections are very important in research and development of a nuclear reactor. The polyethylene (CH_2) is well-known as one of moderator materials to produce a thermal neutron spectrum. The accurate neutron total cross sections of CH_2 are especially important for the evaluation of the neutron flux and the neutron energy spectrum in a nuclear reactor as well as the neutron moderator design. Furthermore, the accurate neutron total cross sections of CH_2 in the thermal neutron energy region (< 1eV) provide important data for the evaluation work on the CH_2 thermal neutron scattering data in the evaluated nuclear data libraries.

In the past, there were a few experiments to obtain the neutron total cross sections of CH_2 using the time-of-flight (TOF) method in the neutron energy range below the MeV region. Herdade *et al.* (1973) [1] measured the total cross sections from 8.2×10^{-4} eV to 0.13 eV using slow chopper with a nuclear reactor. Granada *et al.* (1987) [2] obtained the total cross sections from 0.001 eV to 10 eV using an electron linear accelerator (LINAC) and seven ^{3}He proportional counters. Recently, Lee *et al.* (2002) [3] measured the total cross sections from 0.01 eV to 100 eV at the Pohang Neutron Facility (PNF) using a LINAC to study the possibility to produce nuclear data at the PNF. In the neutron energy region between 100 eV to keV, other experimental data have not been reported.

In the present study, we aim to accurately obtain the neutron total cross sections of CH_2 in the neutron energy range from 0.001 eV to keV region.

To achieve this goal, the transmission measurements of CH_2 were performed by the TOF method at the Kyoto University Institute for Integrated Radiation and Nuclear Science – Linear Accelerator (KURNS-LINAC) using a ^{6}Li detector and a gas electron multiplier (GEM) detector. The obtained neutron total cross sections of CH_2 are compared with the previous measurements and the evaluated data in JENDL-4.0 [4].

2. Experimental method

2.1 Experimental procedure

The transmission measurements of CH_2 were carried out by using the TOF method at the KURNS-LINAC. We have carried out the two different transmission measurements of CH_2 to give a range of energy for the low energy measurement and the high energy measurement. The experimental arrangements for low and high energy measurements are shown in Figures 1 and 2, respectively.

CONTACT Tadafumi Sano t-sano@kindai.ac.jp Institute for Integrated Radiation and Nuclear Science, Kindai University Atomic Energy Research Institute, Kowakae, Higashiosaka-shi, Osaka 577-8502, Japan

This article has been republished with minor changes. These changes do not impact the academic content of the article.

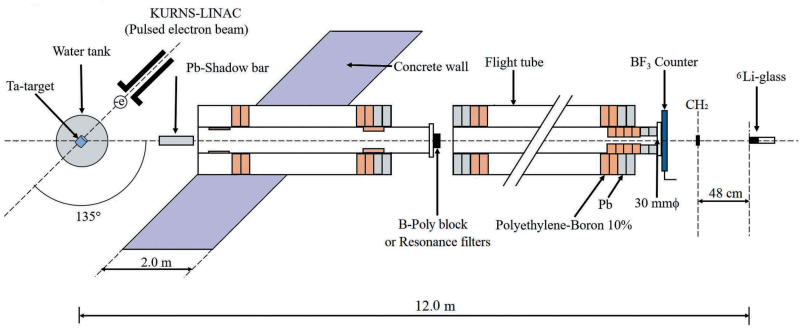

Figure 1. Experimental arrangement for the low energy measurement.

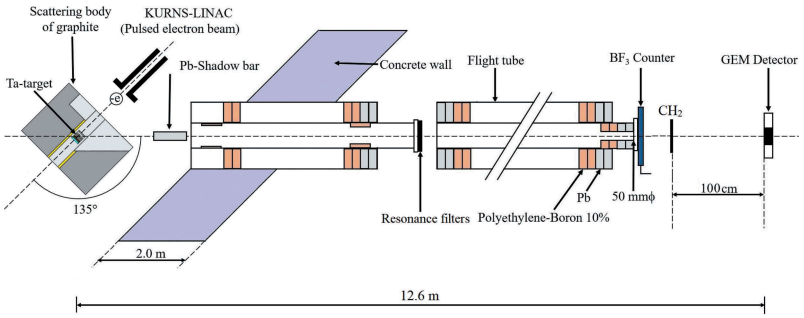

Figure 2. Experimental arrangement for the high energy measurement.

In the low energy measurement, the KURNS-LINAC was operated with a pulse width of 4 μs, a repetition rate of 30 Hz, an average current of 62.5 μA and an electron energy of about 32 MeV. The accelerated electrons struck a water-cooled Ta-target [5] (5 cm in diameter and 6 cm in length), which was composed of 12 sheets of Ta plates with total thickness of 29 mm. The fast neutrons are produced by the photo reaction. To obtain many thermal neutrons, the Ta-target was set at the center of a water moderator tank (20 cm in diameter and 30 cm in high). The neutron flight tube used in the present experiment was in the direction of 135 degrees to the LINAC beam line. A Pb-shadow bar (5 cm in diameter and 20 cm in length) was placed in front of the entrance of the neutron flight tube to reduce the γ-flash generated by the electron burst from the Ta-target. In order to detect the neutrons, a GS20 ^{6}Li glass scintillator (0.5 cm in diameter and 0.5 cm in thickness) was used as a neutron detector. The GS20 ^{6}Li-glass contains enriched ^{6}Li (95%), and the density of the GS20 ^{6}Li-glass is 2.5 g/cm^{3}. The sample was set at 48 cm ahead of the ^{6}Li detector. The distance between the Ta-target and the ^{6}Li detector was about 12 m.

In the high energy measurement, the KURNS-LINAC was operated with a pulse width of 4 μs, a repetition rate of 50 Hz, an average current of 101 μA and an electron energy of about 30 MeV. The photo-neutron target of Ta was used as a pulsed neutron source. To obtain many fast neutrons, the Ta-target was surrounded by a graphite scatterer (50 cm in width, 40 cm in height and thickness) packed in an Al container, 0.5 cm thickness walls, as a target-moderator-reflector system [6]. We used the neutron flight tube of 135 degrees and a Pb-shadow bar (5 cm in diameter and 20 cm in length) as shown in Figure 2. In order to detect the neutrons, the GEM detector (detection area 10 × 10 cm^{2}) having a low sensitivity to γ-rays was used as a neutron detector. A thin-film ^{10}B converter is installed in the GEM detector as a neutron converter. The sample was set at 100 cm ahead of the GEM detector and the distance between the Ta-target and the GEM detector was about 12.5 m.

2.2 Sample and measurement

In the present study, the high-density polyethylene was used to the transmission measurements. The specification of samples is listed in Table 1.

In the low energy measurement, the obtained neutron energy regions were 0.001 to 10 eV. For the

Table 1. Specification of samples.

	Low energy measurement	High energy measurement
Sample name	CH_2	CH_2
Density	0.945 (g/cm^{3})	0.950 (g/cm^{3})
Thickness	4.07 × 10^{-2} (atoms/b), 0.31 (cm)	4.08 × 10^{-2} (atoms/b), 0.20 (cm)
Isotopic composition	99.95%	99.95%
Shape and Size	Plate, 5.06 × 5.06 × 0.31 (cm^{3})	Plate, 20.00 × 20.00 × 0.20 (cm^{3})

detection of the transmitted neutrons from the sample, we employed the ^{6}Li detector. The ^{6}Li detector was operated at −1000 V. Output signals from the ^{6}Li detector were stored in the multi-channel analyzer as the TOF and the pulse height (P.H.) data. In the high energy measurement, the obtained neutron energy regions were 0.01 eV to 40 keV, and the GEM detector was used. The GEM detector was operated with Ar and CO_2 in 70/30 mixing ratio with 90 ml/min flow rate at −2500 V. Output signals from the GEM detector were stored as the TOF data in a personal computer. A block diagrams of the data taking system are shown in Figures 3 and 4, respectively. The neutron beam size is the 3 cm and 5 cm in diameter at the outer entrance of the neutron flight tube for low and high energy measurements.

The incident neutron spectrum was obtained by measuring a TOF spectrum without the sample (blank measurement). To estimate the background level, we have conducted the measurement of the

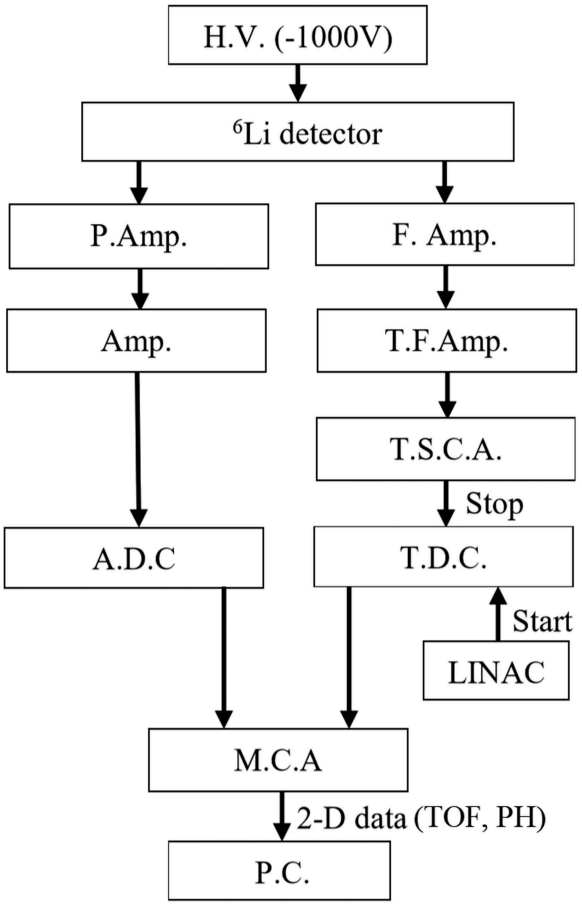

Figure 3. Block diagram for the low energy measurement using the ^{6}Li detector.

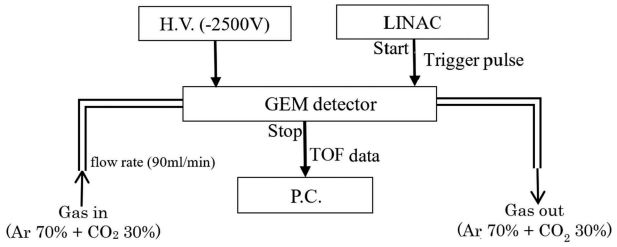

Figure 4. Block diagram for the high energy measurement using the GEM detector.

Table 2. List of measuring times.

Samples	Measurements	Measuring time (h)
Low energy measurement		
Blank	Neutron spectrum	19.4
CH_2	Foreground	13.9
B-Poly Block	Background	3.9
Resonance filters	Energy calibration	1.0
High energy measurement		
Blank	Neutron spectrum	0.5
CH_2	Foreground	0.5
Resonance filters	Background and Energy calibration	0.5

B-Poly block (5 × 10 × 20 cm^3, Boron 10%) or the resonance filters of In, Ag, Co and Mn. The B-Poly block and resonance filters was inserted into the middle of the neutron flight tube as shown in Figures 1 and 2. The energy calibrations were performed with the resonance energies of In (1.46, 3.82 and 9.07 eV), Ag (5.19 and 16.30 eV), Co (132eV) and Mn (336 eV and 2.37 keV). The measuring times are listed in Table 2.

3. Data analysis

In the TOF measurement, the incident neutron energy is expressed as the following equation:

$$E(\mathrm{eV}) = \left(\frac{72.3 \times L(m)}{t(\mu s)}\right)^2 \quad (1)$$

where, E is the incident neutron energy, L is the neutron flight length and t is the TOF.

In the low energy measurement, we obtained the neutron flight length (12.0 m) from the resonance energies at 1.46, 3.82 and 9.07 eV of ^{115}In, 5.19 and 16.30 eV of ^{107}Ag. In the high energy measurement, we obtained the neutron flight length (12.57 m) from the resonance energies at 1.46, 3.82 and 9.07 eV of ^{115}In, 5.19 and 16.30 eV of ^{107}Ag, 132eV of ^{59}Co and 336 eV and 2.37 keV of ^{55}Mn.

The neutron total cross section is determined by measuring the transmitted neutron spectrum through the sample and comparing the incident neutron spectrum. The relation between the neutron transmission $T(E)$ and the neutron total cross section $\sigma_{tot}(E)$ is defined as follows:

$$T(E) = \frac{\varphi_{out}(E)}{\varphi_{in}(E)} = \exp(-n \cdot \sigma_{tot}(E)) \qquad (2)$$

where, φ_{in} is the incident neutron spectrum in the open beam, φ_{out} is the transmitted neutron spectrum through the sample. n is the thickness of the sample, atoms/b.

In the present experiments, the neutron total cross section $\sigma_{tot}(E)$ was obtained by the following equation:

$$\sigma_{tot}(E) = -\frac{1}{n} \cdot \mathrm{In}(T(E)) = -\frac{1}{n} \cdot \mathrm{In}\frac{C_{in}(E) - C_{back}(E)}{C_{out}(E) - C_{back}(E)} \qquad (3)$$

where, $C_{out}(E)$ and $C_{in}(E)$ are the neutron count rates for the sample-out and sample-in. $C_{back}(E)$ is the background. The sample-out and sample-in TOF spectra in the low and high energy measurements are shown in Figures 5 and 6, respectively.

In the high energy measurement, the background level was estimated by using the resonance peaks at 1.46 eV, 5.19 eV, 132eV and 336 eV. To derive the continues background level, the count rates at the black resonances were interpolated by using the

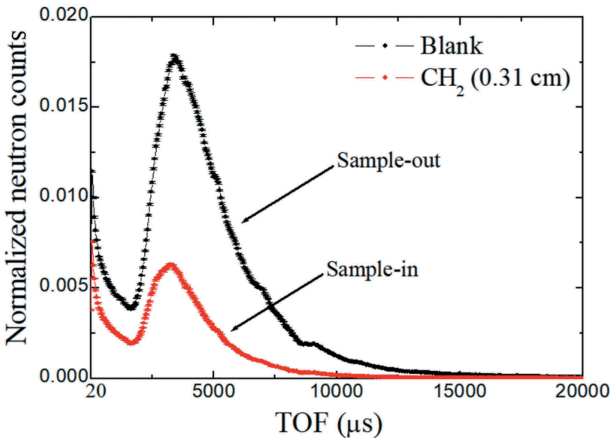

Figure 5. Sample-out and sample-in TOF spectra in the low energy measurement.

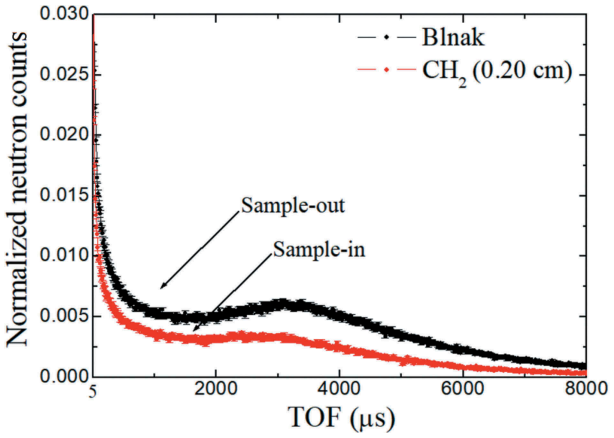

Figure 6. Sample-out and sample-in TOF spectra in the high energy measurement.

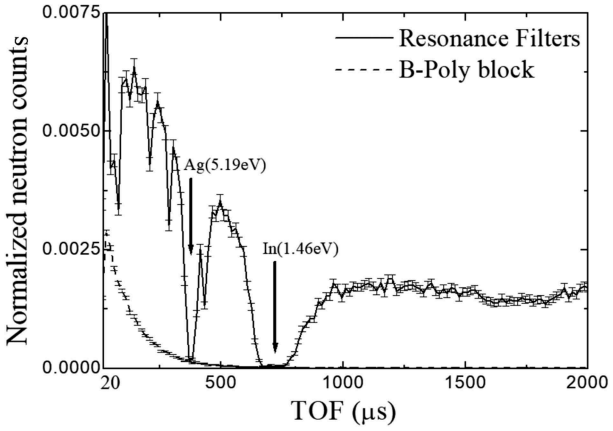

Figure 7. Background level obtained by the B-Ploy block measurement in the low energy measurement.

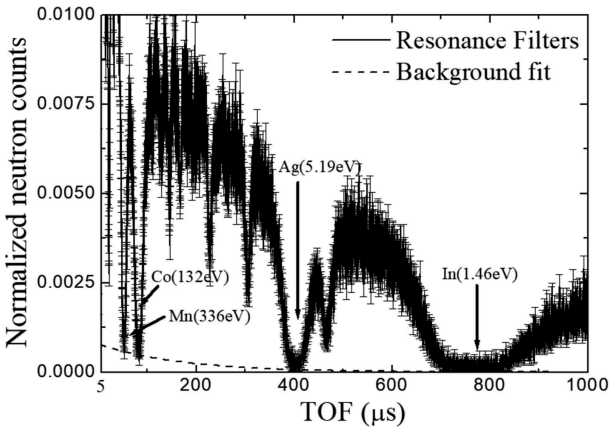

Figure 8. Background level estimated by using the resonance peaks in the high energy measurement.

fitting equation $C_{back}(t) = A_1 + A_2.\exp(-A_3.t)$. where, $C_{back}(t)$ is the background at the time t and $A_1 \sim A_3$ are the fitting parameters.

In the low energy measurement, since we were only able to get the two resonance peaks at 1.46 eV and 5.19e V available for the fitting equation $C_{back}(t)$, it is difficult to derive the continues background level using the fitting. To investigate the continues background level, we have carried out the measurement of the B-Poly block, and the B-Ploy block was used as a neutron absorber. From the measured results of the B-Poly block, we can obtain the continues background level. The background levels in the low and high energy measurements are shown in Figures 7 and 8.

In the present measurements, the dead times of the detector and electronics were considered to be negligible because they were estimated to be < 0.1%.

4. Uncertainties

In the present transmission measurements, the following uncertainties were taken into account: the statistical uncertainties of TOF spectrum and systematic uncertainties such as the neutron flight

Table 3. Experimental uncertainties.

	Low energy measurement	High energy measurement
Statistical uncertainties	0.001–0.01 eV, 0.3 – 3.1% 0.01–0.1 eV, 0.2 – 0.4% 0.1–1 eV, 0.4 – 1.3% 1–10 eV, 1.2 – 2.2%	0.01 – 1 eV, 0.6 – 2.4% 1 – 100 eV, 1.3 – 3.1% 100 eV–10 keV, 3.0 – 6.0% 10 – 40 keV, 4.8 – 5.1%
Systematic uncertainties		
Uncertainty of neutron flight length	< 0.3%	< 0.3%
Uncertainty of sample thickness	–	–
Uncertainty of background fitting	–	< 0.3%
Uncertainty of dead time	–	–
Effect of in-scattering	< 1%	< 1%

length, the sample thickness, the background fitting, the dead time and the in-scattering effect. The experimental uncertainties are summarized in Table 3.

The statistical uncertainties were about 0.2% to 3.1% for the low energy measurement and about 0.6% to 6% for the high energy measurement. The neutron flight lengths were obtained by fitting neutron TOF and corresponding to the resonance energy. The systematic uncertainties due to the neutron flight length were estimated less than 0.3%. The systematic uncertainties due to the sample thickness were consider as negligible small. For the high energy measurement, the systematic uncertainties from the background fitting affecting the total cross sections of CH_2 was less than about 0.3%. The dead time from the detector and electronics could be neglected in the present experiments.

In the present measurements, the in-scattering effect was considered as the systematic uncertainty and this effect is calculated by the MCNP5 [7] with JENDL-4.0. In this calculation, the sample size, the neutron beam size and the incident neutron spectrum were considered to be same as the experimental conditions. The in-scattering effect was obtained by comparing the neutron spectrum at 0.48 m (or 1 m) with 10 m after passing the CH_2 sample.

The total uncertainties were about 0.5% to 3.3% for the low energy measurement and about 1.7% to 7.5% for the high energy measurement. The obtained total uncertainties are shown in Figure 9.

5. Results and discussion

In the present experiments, we have acquired the neutron total cross sections of CH_2 in the neutron energy region from 0.001 and 10 eV and from 0.01 eV to 40 keV. The present results are compared

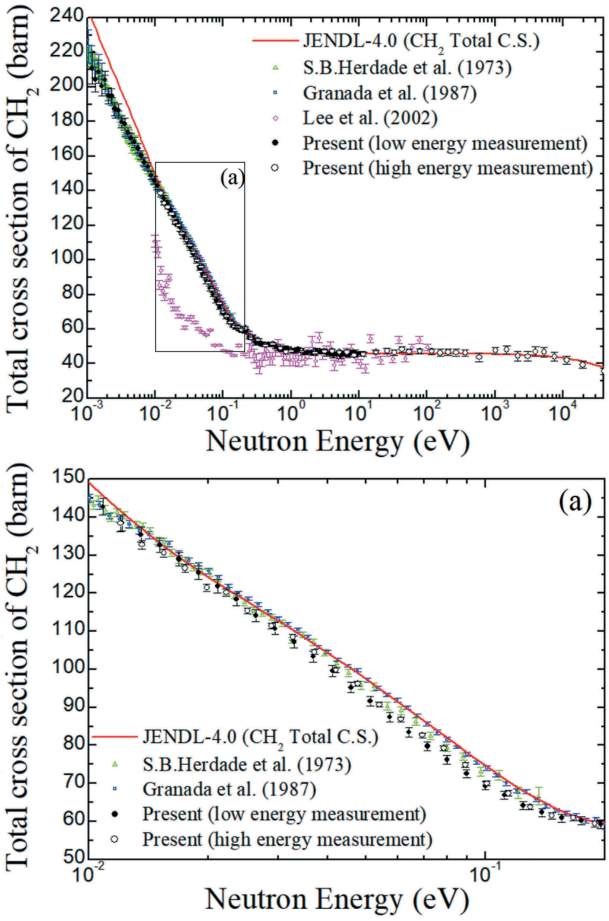

Figure 9. Comparison of the present results with the previous measured results and the evaluated data for the neutron total cross sections of CH_2.

with the previous results and the evaluated data in JENDL-4.0 as shown in Figure 9. The numerical data of the present results are listed in Tables 4 and 5.

In the low energy measurement, the experimental data of Herdade *et al.* [1] and Granada *et al.* [2] show good agreement with the present results in the neutron energy region from 0.001 and 0.01 eV. On the other hand, the evaluated data in JENDL-4.0 are larger than the present results and the previous results as shown in Figure 9. A discrepancy between the evaluated data and the measured results is thought to have been caused by the thermal neutron scattering law of CH_2 in the evaluated nuclear data. For the neutron energy region from 0.035 to 0.15 eV, the experimental data of Granada *et al.* [2] and the evaluated data in JENDL-4.0 are up to about 6% larger than the present results.

In the high energy measurement, the experimental data of Granada *et al.* [2] and the evaluated data in JENDL-4.0 are up to about 4% larger than the present results in the energy region from 0.035 to 0.15 eV. For the neutron energy region from 100 eV to 40 keV, we have supplied the first experimental data of CH_2. The evaluated data in JENDL-4.0 are in good agreement with the present results within the error range.

Table 4. Numerical data of the neutron total cross sections of CH_2 for the low energy measurement.

	Neutron energy interval (eV)		Average neutron energy (eV)	Average total cross section (b)	Error (b)
	E_n [lower]	E_n [upper]			
1	1.119E-03	1.250E-03	1.181E-03	2.108E+02	6.861E+00
2	1.250E-03	1.399E-03	1.321E-03	2.043E+02	5.163E+00
3	1.399E-03	1.558E-03	1.475E-03	2.087E+02	4.523E+00
4	1.558E-03	1.738E-03	1.644E-03	2.005E+02	3.750E+00
5	1.738E-03	1.948E-03	1.838E-03	2.040E+02	3.266E+00
6	1.948E-03	2.178E-03	2.058E-03	1.948E+02	2.700E+00
7	2.178E-03	2.426E-03	2.297E-03	1.947E+02	2.428E+00
8	2.426E-03	2.718E-03	2.566E-03	1.872E+02	2.178E+00
9	2.718E-03	3.035E-03	2.870E-03	1.863E+02	2.002E+00
10	3.035E-03	3.388E-03	3.204E-03	1.798E+02	1.791E+00
11	3.388E-03	3.789E-03	3.580E-03	1.785E+02	1.680E+00
12	3.789E-03	4.235E-03	4.003E-03	1.735E+02	1.502E+00
13	4.235E-03	4.728E-03	4.472E-03	1.702E+02	1.406E+00
14	4.728E-03	5.283E-03	4.994E-03	1.680E+02	1.277E+00
15	5.283E-03	5.909E-03	5.583E-03	1.644E+02	1.137E+00
16	5.909E-03	6.591E-03	6.236E-03	1.605E+02	1.040E+00
17	6.591E-03	7.375E-03	6.967E-03	1.562E+02	9.535E-01
18	7.375E-03	8.252E-03	7.795E-03	1.539E+02	8.699E-01
19	8.252E-03	9.228E-03	8.720E-03	1.490E+02	8.021E-01
20	9.228E-03	1.031E-02	9.746E-03	1.459E+02	7.920E-01
21	1.031E-02	1.150E-02	1.088E-02	1.427E+02	7.324E-01
22	1.150E-02	1.285E-02	1.215E-02	1.385E+02	6.633E-01
23	1.285E-02	1.433E-02	1.356E-02	1.354E+02	6.269E-01
24	1.433E-02	1.601E-02	1.514E-02	1.327E+02	5.880E-01
25	1.601E-02	1.790E-02	1.692E-02	1.290E+02	5.648E-01
26	1.790E-02	2.005E-02	1.893E-02	1.254E+02	5.357E-01
27	2.005E-02	2.236E-02	2.116E-02	1.219E+02	5.123E-01
28	2.236E-02	2.494E-02	2.359E-02	1.184E+02	4.895E-01
29	2.494E-02	2.799E-02	2.640E-02	1.141E+02	4.542E-01
30	2.799E-02	3.122E-02	2.954E-02	1.107E+02	4.439E-01
31	3.122E-02	3.481E-02	3.294E-02	1.072E+02	4.286E-01
32	3.481E-02	3.904E-02	3.683E-02	1.033E+02	4.048E-01
33	3.904E-02	4.342E-02	4.114E-02	9.959E+01	3.991E-01
34	4.342E-02	4.857E-02	4.589E-02	9.520E+01	3.803E-01
35	4.857E-02	5.423E-02	5.129E-02	9.156E+01	3.734E-01
36	5.423E-02	6.094E-02	5.744E-02	8.738E+01	3.566E-01
37	6.094E-02	6.763E-02	6.415E-02	8.346E+01	3.599E-01
38	6.763E-02	7.549E-02	7.140E-02	7.980E+01	3.527E-01
39	7.549E-02	8.481E-02	7.995E-02	7.624E+01	3.496E-01
40	8.481E-02	9.486E-02	8.962E-02	7.250E+01	3.574E-01
41	9.486E-02	1.055E-01	9.998E-02	6.935E+01	3.696E-01
42	1.055E-01	1.181E-01	1.115E-01	6.693E+01	3.776E-01
43	1.181E-01	1.312E-01	1.244E-01	6.422E+01	4.057E-01
44	1.312E-01	1.467E-01	1.386E-01	6.236E+01	4.284E-01
45	1.467E-01	1.651E-01	1.555E-01	6.089E+01	4.569E-01
46	1.651E-01	1.841E-01	1.742E-01	6.019E+01	5.143E-01
47	1.841E-01	2.067E-01	1.949E-01	5.929E+01	5.423E-01
48	2.067E-01	2.295E-01	2.177E-01	5.883E+01	5.966E-01
49	2.295E-01	2.564E-01	2.424E-01	5.539E+01	5.964E-01
50	2.564E-01	2.882E-01	2.716E-01	5.497E+01	6.012E-01
51	2.882E-01	3.194E-01	3.032E-01	5.209E+01	6.294E-01
52	3.194E-01	3.561E-01	3.370E-01	5.205E+01	6.236E-01
53	3.561E-01	3.994E-01	3.768E-01	5.134E+01	6.116E-01
54	3.994E-01	4.401E-01	4.190E-01	5.098E+01	6.608E-01
55	4.401E-01	5.002E-01	4.687E-01	5.090E+01	5.983E-01
56	5.002E-01	5.576E-01	5.277E-01	5.071E+01	6.548E-01
57	5.576E-01	6.256E-01	5.901E-01	5.018E+01	6.453E-01
58	6.256E-01	6.850E-01	6.543E-01	4.876E+01	7.143E-01
59	6.850E-01	7.784E-01	7.295E-01	4.828E+01	6.279E-01
60	7.784E-01	8.616E-01	8.184E-01	4.895E+01	7.036E-01
61	8.616E-01	9.589E-01	9.083E-01	4.857E+01	6.943E-01
62	9.589E-01	1.074E+00	1.014E+00	4.789E+01	6.855E-01
63	1.074E+00	1.210E+00	1.139E+00	4.719E+01	6.785E-01
64	1.210E+00	1.316E+00	1.262E+00	4.824E+01	8.042E-01
65	1.316E+00	1.504E+00	1.405E+00	4.788E+01	6.700E-01
66	1.504E+00	1.652E+00	1.575E+00	4.625E+01	7.857E-01
67	1.652E+00	1.823E+00	1.734E+00	4.643E+01	7.814E-01
68	1.823E+00	2.134E+00	1.969E+00	4.650E+01	6.498E-01
69	2.134E+00	2.255E+00	2.193E+00	4.620E+01	1.050E+00
70	2.255E+00	2.532E+00	2.388E+00	4.767E+01	7.796E-01
71	2.532E+00	2.863E+00	2.690E+00	4.685E+01	7.676E-01
72	2.863E+00	3.262E+00	3.053E+00	4.725E+01	7.675E-01
73	3.262E+00	3.495E+00	3.376E+00	4.571E+01	1.036E+00
74	3.495E+00	4.040E+00	3.752E+00	4.572E+01	7.570E-01
75	4.040E+00	4.362E+00	4.196E+00	4.482E+01	1.035E+00
76	4.362E+00	5.132E+00	4.723E+00	4.527E+01	7.570E-01

(*Continued*)

Table 4. (Continued).

	Neutron energy interval (eV)		Average neutron energy (eV)	Average total cross section (b)	Error (b)
	E_n [lower]	E_n [upper]			
77	5.132E+00	5.596E+00	5.357E+00	4.433E+01	1.034E+00
78	5.596E+00	6.126E+00	5.852E+00	4.555E+01	1.038E+00
79	6.126E+00	6.735E+00	6.420E+00	4.564E+01	1.049E+00
80	6.735E+00	7.440E+00	7.075E+00	4.507E+01	1.051E+00
81	7.440E+00	8.261E+00	7.835E+00	4.627E+01	1.065E+00
82	8.261E+00	9.227E+00	8.724E+00	4.652E+01	1.076E+00
83	9.227E+00	1.037E+01	9.774E+00	4.574E+01	1.079E+00
84	1.037E+01	1.174E+01	1.103E+01	4.560E+01	1.065E+00

Table 5. Numerical data of the neutron total cross sections of CH_2 for the high energy measurement.

	Neutron energy interval (eV)		Average neutron energy (eV)	Average total cross section (b)	Error (b)
	E_n [lower]	E_n [upper]			
1	1.133E-02	1.284E-02	1.205E-02	1.384E+02	2.176E+00
2	1.284E-02	1.455E-02	1.366E-02	1.328E+02	2.506E+00
3	1.455E-02	1.650E-02	1.548E-02	1.305E+02	2.392E+00
4	1.650E-02	1.868E-02	1.754E-02	1.266E+02	2.272E+00
5	1.868E-02	2.118E-02	1.987E-02	1.215E+02	2.137E+00
6	2.118E-02	2.338E-02	2.224E-02	1.202E+02	2.185E+00
7	2.338E-02	2.717E-02	2.517E-02	1.153E+02	1.897E+00
8	2.717E-02	3.079E-02	2.890E-02	1.114E+02	1.877E+00
9	3.079E-02	3.490E-02	3.275E-02	1.085E+02	1.809E+00
10	3.490E-02	3.953E-02	3.711E-02	1.045E+02	1.741E+00
11	3.953E-02	4.482E-02	4.205E-02	9.980E+01	1.669E+00
12	4.482E-02	5.079E-02	4.766E-02	9.617E+01	1.611E+00
13	5.079E-02	5.754E-02	5.401E-02	9.067E+01	1.546E+00
14	5.754E-02	6.522E-02	6.120E-02	8.688E+01	1.498E+00
15	6.522E-02	7.384E-02	6.933E-02	8.270E+01	1.457E+00
16	7.384E-02	8.375E-02	7.856E-02	7.929E+01	1.430E+00
17	8.375E-02	9.488E-02	8.905E-02	7.487E+01	1.397E+00
18	9.488E-02	1.075E-01	1.009E-01	6.999E+01	1.366E+00
19	1.075E-01	1.218E-01	1.143E-01	6.735E+01	1.367E+00
20	1.218E-01	1.380E-01	1.295E-01	6.373E+01	1.349E+00
21	1.380E-01	1.564E-01	1.468E-01	6.145E+01	1.362E+00
22	1.564E-01	1.773E-01	1.664E-01	6.093E+01	1.372E+00
23	1.773E-01	2.008E-01	1.885E-01	5.939E+01	1.404E+00
24	2.008E-01	2.278E-01	2.137E-01	6.044E+01	1.449E+00
25	2.278E-01	2.919E-01	2.569E-01	5.477E+01	1.174E+00
26	2.919E-01	3.751E-01	3.296E-01	5.353E+01	1.197E+00
27	3.751E-01	4.814E-01	4.233E-01	5.059E+01	1.211E+00
28	4.814E-01	6.182E-01	5.434E-01	5.135E+01	1.251E+00
29	6.182E-01	7.942E-01	6.980E-01	4.885E+01	1.252E+00
30	7.942E-01	9.003E-01	8.448E-01	4.672E+01	1.605E+00
31	9.003E-01	1.155E+00	1.016E+00	4.730E+01	1.300E+00
32	1.155E+00	1.898E+00	1.458E+00	4.703E+01	1.094E+00
33	1.898E+00	2.774E+00	2.274E+00	4.625E+01	1.251E+00
34	2.774E+00	3.560E+00	3.130E+00	4.699E+01	1.493E+00
35	3.560E+00	4.602E+00	4.031E+00	4.735E+01	1.533E+00
36	4.602E+00	5.917E+00	5.198E+00	4.649E+01	1.579E+00
37	5.917E+00	7.603E+00	6.681E+00	4.659E+01	1.640E+00
38	7.603E+00	9.714E+00	8.562E+00	4.478E+01	1.661E+00
39	9.714E+00	1.415E+01	1.162E+01	4.541E+01	1.553E+00
40	1.415E+01	2.299E+01	1.777E+01	4.653E+01	1.545E+00
41	2.299E+01	2.942E+01	2.591E+01	4.722E+01	2.025E+00
42	2.942E+01	3.794E+01	3.328E+01	4.633E+01	2.103E+00
43	3.794E+01	4.922E+01	4.303E+01	4.814E+01	2.107E+00
44	4.922E+01	6.188E+01	5.501E+01	4.684E+01	2.149E+00
45	6.188E+01	1.030E+02	7.857E+01	4.710E+01	1.857E+00
46	1.030E+02	1.374E+02	1.184E+02	4.693E+01	2.160E+00
47	1.374E+02	1.812E+02	1.570E+02	4.614E+01	2.536E+00
48	1.812E+02	2.332E+02	2.047E+02	4.647E+01	2.306E+00
49	2.332E+02	3.112E+02	2.680E+02	4.628E+01	2.434E+00
50	3.112E+02	4.362E+02	3.658E+02	4.612E+01	2.401E+00
51	4.362E+02	8.319E+02	5.870E+02	4.362E+01	2.910E+00
52	8.319E+02	1.269E+03	1.016E+03	4.752E+01	2.411E+00
53	1.269E+03	1.786E+03	1.495E+03	4.795E+01	2.689E+00
54	1.786E+03	2.695E+03	2.171E+03	4.431E+01	3.327E+00
55	2.695E+03	3.436E+03	3.032E+03	4.416E+01	3.284E+00
56	3.436E+03	4.529E+03	3.926E+03	4.686E+01	3.234E+00
57	4.529E+03	6.242E+03	5.283E+03	4.658E+01	3.144E+00
58	6.242E+03	9.146E+03	7.487E+03	4.387E+01	2.950E+00
59	9.146E+03	1.467E+04	1.142E+04	4.208E+01	2.713E+00
60	1.467E+04	2.729E+04	1.954E+04	3.932E+01	2.480E+00
61	2.729E+04	6.738E+04	4.076E+04	3.556E+01	2.165E+00

Furthermore, the low energy measurement results were in good agreement with the high energy one within the experimental error. The experimental data of Lee *et al.* [3] are largely different from others measured data in the energy region below 0.5 eV.

6. Conclusions

We have performed the neutron total cross section measurements of CH_2 using TOF method at the KURNS-LINAC. The obtained neutron energy ranges were 0.001 eV to 40 keV. The measured results were compared with the previous experimental results and the evaluated data in JENDL-4.0.

In the energy range below 0.01eV, the present results indicate that evaluated data in JENDL-4.0 are overestimated. In the energy range from 0.035 to 0.15 eV, the data by Granada *et al.* [2] and the evaluated data in JENDL-4.0 are up to about 4 ~ 6% larger than the present results.

The two measured results using ^{6}Li detector and the GEM detector are in good agreement within experimental error. From this result, we can cross-check the validity of the present data.

Moreover, the neutron total cross sections of CH_2 were first time measured in the neutron energy region from 100 eV and 40 keV by using TOF method.

Acknowledgments

The authors would like to express their sincere thanks to all the staff of the Kyoto University Institute for Integrated Radiation and Nuclear Science - Linear Accelerator (KURNS-LINAC) for making it possible to operate excellently the LINAC. Then, special thanks to IWAO for the assistance with a research idea.

This research is a collaborative effort of the Toshiba Energy Systems & Solutions, the Tokyo Institute of Technology and the Kyoto University. A part of this study was supported by Toshiba Energy Systems & Solutions Corporation.

This work was supported by the Toshiba Energy System and Solution Corporation.

Disclosure statement

No potential conflict of interest was reported by the authors.

References

[1] Herdade SB, Vinhas LA, Rodrigues C, et al. Neutron cross sections of polyethylene and light water in the energy range 8.2×10^{-4} to 0.13 eV. Brazil: Brazilian Atomic Energy Commission and Institute of Physics report to the IEA; 1973. (Report no.310).

[2] Granada JR, Dawidowski J, Mayer RE, et al. Thermal neutron cross section and transport properties of polyethylene. Nucl Instrum Methods A. 1987; 261:573–578.

[3] Lee YS, Cho MH, Ko IS, et al. The status of neutron total cross-section measurement by using 100-MeV electron linear accelerator for nuclear data production in Korea. Radiat Meas. 2002;35:321–326.

[4] Shibata K, Iwamoto O, Nakagawa T, et al. JENDL-4.0: A new library for nuclear science and engineering. J Nucl Sci Technol. 2011;48:1–30.

[5] Kobayashi K, Jin G, Yamamoto S, et al. KURRI-LINAC as a Neutron Source for Irradiation. Osaka: Research Reactor Institute of Kyoto University; 1987. (Report no.22).

[6] Takahashi Y, Kiyanagi Y, Watanabe K, et al. Development of a neutron source for imaging at the electron linac facility in Kyoto University research reactor institute. Phys B Condens Matter. 2018;551:488–491.

[7] X-5 Monte Carlo Team. MCNP, General Monte Carlo N-Particle Transport Code, Version 5. Los Alamos National Laboratory; 2003. LA-UR-03-1987.